Philipp Fricker*
Matthias Baumann
Frank Bauer

How Wetting Properties Influence the Wear of Radial Lip Sealing Systems

Increased wear on radial lip seal systems is observed when sealing modern lubricants, such as polyglycols and esters. This can impair the function of the sealing system and ultimately lead to leakage. This work, carried out within the AiF research project "Welleneinlauf" (wear of counter faces) [1], shows methods to identify and predict excessive wear of radial lip sealing systems based on their wetting properties and pumping rate. The knowledge gained will support users by providing faster and more cost-effective testing methods early in the design process, thus enables a significant increase in the service life of radial lip sealing systems.

Keywords: Lubricants, Radial lip seal, Wear, Wetting properties

Received: August 07, 2022; *revised:* September 11, 2022; *accepted:* September 23, 2022

DOI: 10.1002/ceat.202200375

Supporting Information available online

1 Introduction

Sealing systems prevent fluid exchange between separated functional areas in technical applications due to an active back-pumping mechanism that is able to pump lubricant from the air to the oil side. An overview of the principles and hypotheses involved is given by Bauer [2]. This function must be guaranteed permanently or at least in the long term to maintain the product functionality. Wear and tear – which increases over the operating period – leads at some point to the failure of the sealing system. The consequences of unintended failure range from damage to the manufacturer's reputation, to environmental damage, and to economic damage due to the unavailability of machines and plants.

In addition to the geometry of the sealing edge – the part of the radial lip seal, which contacts the sealing counter face – the designer can create a radial lip sealing system, as shown in Fig. 1, according to the seal material, the production method, and the surface finish of the shaft counter face. The suitability of the elastomer-counter face fluid compatibility can so far only be determined with experimental tests after trial and error. Chemical compatibility data, provided by the sealing manufacturer, can only be used as a guideline, but says nothing about the suitability of the lubricant as wear protection during operation.

Current research from several areas of tribology, carried out by Kretschmer [4], Kalin [5, 6], and Bobzin [7], points to a connection between wetting properties and the wear of friction partners. For seals, this approach was first pursued at the Institute of Machine Components by Klaiber [8] and Schuler [9].

Like every tribological system, the radial lip sealing system is exposed to wear. Wear occurs on the radial lip seal, the shaft counter face, and even the lubricant is affected. During operation, a hydrodynamic lubricant film forms between the radial lip seal and the counter face, which causes the sealing edge to be lifted of the counter face. A fluid-filled sealing gap with a specific gap height emerges, thus, considerably reducing wear. The variables that influence the gap height (fluid viscosity η[1)], angular velocity ω, and average pressure p_m in the sealing gap) are summarized in the unitless duty parameter G given in Eq. (1).

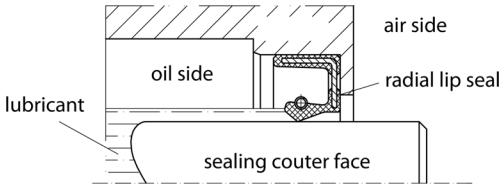

Figure 1. Installed radial lip sealing system .

$$G = \eta \omega p_m^{-1} \tag{1}$$

For $G \geq 10^{-7}$ predominantly fluid friction is assumed. Therefore, radial lip seals should hardly wear at all if the speed is high enough and the lubricant supply is sufficient. For particle-free mineral oils this assumption is largely correct. However, chemically different lubricants (polyglycols, poly-α-olefins, esters) of the same viscosity class, often deviate considerably from this previous assumption. As current work [3–10] demonstrates, the wetting properties of the lubricants are decisive.

In this paper, the wetting and material properties of eleven commercially available lubricants of different base oils and

1) List of symbols at the end of the paper.

Philipp Fricker, Dr.-Ing. Matthias Baumann, Dr.-Ing. Frank Bauer
Philipp.fricker@web.de
University of Stuttgart, Institute of Machine Components (IMA), Research Department Sealing Technology, Pfaffenwaldring 9, 70569 Stuttgart, Germany.

viscosity classes were analyzed (two mineral oils, two poly-α-olefins, four polyglycols, two esters, one silicone oil) and wear tests were carried out on real sealing systems consisting of polished 100Cr6 counter faces and radial lip seals made of 75FKM585 elastomer. Furthermore, it is illustrated how the wear behavior of sealing systems can be predicted by a combined consideration of wetting properties (spreading coefficient, penetrativity) with functional properties such as the pumping rate of a radial lip sealing system.

2 State of the Art

2.1 Interfacial Tension

An interface is created when two substances or phases come into contact. In the contact zone, intermolecular forces act, which cause an interaction between the substances or phases involved. According to Dörfler [11], these interactions are called interfacial tension.

The interfacial tension σ_{ab} can simply be seen as an attraction force between the substances a and b in contact and can be divided in two partitions. One is an inward force on the surface molecules causing the liquid to contract. The second one is a tangential force parallel to the surface of the liquid. This tangential force is generally referred to as the surface tension.

According to Fowkes [12], the surface tension of each material is composed of a disperse component σ_d (also known as Van der Waals forces, caused by London forces) and a polar component σ_p (mainly caused by dipoles, hydrogen bonds, ions, electrons). This is indicated in Eq. (2).

$$\sigma = \sigma_d + \sigma_p \tag{2}$$

Taking into account the geometric mean of the surface tensions σ_a and σ_b according to Owens and Wendt [13], the interfacial tension σ_{ab} can be determined using Eq. (3).

$$\sigma_{ab} = \sigma_a + \sigma_b - 2\sqrt{\sigma_a^d \sigma_b^d} - 2\sqrt{\sigma_a^p \sigma_b^p} \tag{3}$$

Rabel [14] transformed Eq. (3) to a straight line form. Thus, the disperse and polar components of the surface tension of a solid σ_s could be determined for the first time by conducting two measurements with different measuring liquids using the sessile drop method, explained in Section 3.1.2.

Kaelble [15] substituted the interfacial tension σ_{ab} with the work of adhesion W_a and obtained Eq. (4). This allows the work of adhesion (which can be described as the bound energy during wetting between a solid and liquid phase) between a solid s and a liquid l to be calculated mathematically directly from the corresponding surface tensions σ_s and σ_l.

$$W_a = 2\left(\sqrt{\sigma_s^d}\sqrt{\sigma_l^d} + \sqrt{\sigma_s^p}\sqrt{\sigma_l^p}\right) \tag{4}$$

The calculation method is standardized in DIN 55660-2 [16] and is abbreviated OWRK (Owens, Wendt, Rabel, and Kaeble).

For determining the work of adhesion, Wu [17] proposes the harmonic mean, defined in Eq. (5), instead of the geometric mean. He investigated polymer melts that did not mix with each other. The interfacial tension σ_{ab} could be measured directly. Thereby he noticed deviations from the calculation method according to OWRK.

$$\sigma_{ab} = \sigma_a + \sigma_b - 2\frac{2\sigma_a^d \sigma_b^d}{\sigma_a^d + \sigma_b^d} - 2\frac{2\sigma_a^p \sigma_b^p}{\sigma_a^p + \sigma_b^p} \tag{5}$$

The work of adhesion results in Eq. (6).

$$W_a = 2\left(\frac{2\sigma_a^d \sigma_b^d}{\sigma_a^d + \sigma_b^d} + \frac{2\sigma_a^p \sigma_b^p}{\sigma_a^p + \sigma_b^p}\right) \tag{6}$$

The calculation method according to Wu is also standardized in DIN 55660-2 [16] and is recommended for low-energy surfaces with $\sigma < 20\,\mathrm{Nm^{-1}10^{-3}}$.

2.1.1 Spreading Coefficient

Harkins and Feldman [18] introduced a measure for the wettability of solid surfaces by liquids. They defined the spreading coefficient S as the difference between the work of adhesion W_a and the work of cohesion W_c; the work of cohesion can be described as the bound energy between two surfaces of the same liquid. The work of cohesion is defined in Eq. (7) as double the surface tension of the regarded liquid.

$$W_c = 2\sigma_l \tag{7}$$

With the work of cohesion, the spreading coefficient S can be calculated using Eq. (8).

$$S = W_a - W_c \tag{8}$$

Harkins and Feldman [18] assume complete wetting for spreading coefficients $S > 0$. For spreading coefficients $S < 0$ incomplete wetting occurs.

2.1.2 Young-Laplace Equation

According to Wolf [19],the curvature of the liquid surface of a drop depends on its surface tension σ_l and the differential pressure Δp to the surrounding phase. The mathematical description is provided by the Young-Laplace equation in Eq. (9). r_1 and r_2 are the two main radii of the curved drop.

$$\Delta p = \sigma_l\left(\frac{1}{r_1} + \frac{1}{r_2}\right) \tag{9}$$

2.1.3 Penetrativity

Liquids naturally penetrate narrow horizontal and vertical gaps. In vertical gaps, the penetration height is limited by gravity. In horizontal gaps, the penetration length of a liquid is limited only by the available volume. This effect is due to the curvature of the liquid surface, which is described by the Young-Laplace equation (Eq. (9)). The penetration length of a liquid into a narrow gap also depends on time. Washburn [20]

summarized the dependency of the penetration velocity on the surface tension σ_l, the contact angle θ, and the viscosity η in Eq. (10), the penetrativity Ψ.

$$\Psi = \frac{\sigma_l \cos\theta}{2\eta} \tag{10}$$

According to Schuler [9], the penetrativity for horizontal annular gaps with walls made of two different materials can be approximated using Eq. (11).

$$\Psi \approx \frac{\sigma_l \cos\left(\frac{\theta_1+\theta_2}{2}\right)}{2\eta} \tag{11}$$

3 Methods

3.1 Measuring Instruments

3.1.1 Bubble Pressure Tensiometer

A bubble pressure tensiometer SITA SCIENCE LINE T60 was used to determine the surface tension of the liquids. The measuring principle is based on the Young-Laplace equation. A dried air stream is blown into the liquid through a capillary. Gas bubbles form at the tip, whose surface becomes more and more curved as the volume increases. Simultaneously the bubble radius decreases. From bubble formation to bubble detachment, the bubble pressure passes a characteristic pressure curve from which the surface tension of the surrounding liquid is calculated. The maximum pressure is reached at the smallest bubble radius, with the gas bubble having the shape of a hemisphere. As the process progresses, the bubble radius increases rapidly and the bubble pressure drops, causing it to detach. The surface tension σ_l of the liquid is determined from the measured maximum pressure $\hat{p}$ and the known capillary diameter d_{cap}. The maximum pressure is equalized with the capillary pressure and the hydrostatic pressure.

$$\hat{p} = \frac{4\sigma_l}{d_{cap}} + g\rho h_t \tag{12}$$

3.1.2 Sessile Drop Method

A DataPhysics OCA20 contact angle measurement system was used to determine the surface tension of the solids. Drops of at least two different test liquids (the disperse and polar fraction of the surface tension must be known) are successively deposited on the solid. In the static state the contour of the drop is determined. The contact angle is found by applying tangents to the drop contour at the two intersections with the base line (common phase boundary between drop and substrate). With the help of the contact angle, the disperse and polar fractions of the surface tension of the substrate can be assessed mathematically according to OWRK and Wu. The calculation methods are standardized in DIN 55660-2 [16].

To increase the accuracy of the measurements, three measuring fluids were used. The values of the disperse and polar fractions of the surface tension of each fluid are shown in the Supporting Information S1.

3.1.3 Pendant Drop Method

A DataPhysics OCA20 contact angle measurement system was used to determine the polar and disperse fraction of the surface tension of the liquids.

A needle creates a pendant drop of a reference liquid in the liquid to be tested. According to the Young-Laplace equation, the characteristic shape of the pendant drop results in an interfacial tension between the liquid to be tested and the reference liquid. Together with the known surface tension of the reference liquid and the test liquid, the disperse fraction of the surface energy can be determined mathematically according to OWRK or Wu. The calculation methods are standardized in DIN 55660-4 [21]. As a reference liquid, purely disperse perfluoro octane ($\sigma_p = 14\,\mathrm{Nm^{-1}10^{-3}}$, Ström [22]) has been used for the results shown later in this paper.

3.1.4 Tactile Surface Measurement

A tactile Hommel T8000 measurement instrument was used to measure the length and the depth of the wear track on the shaft counter faces after each test run. For this purpose, the shaft is clamped in a chuck. The texture of the surface and its roughness are measured by means of an axially movable stylus.

3.1.5 IMA-Sealobserver®

An IMA-Sealobserver® was employed in conjunction with a digital microscope to take high-resolution photographs of the radial lip seals worn sealing edges. The IMA-Sealobserver® thereby deflects the beam path of the microscope, ensures a defined position, and provides consistent illumination of the sealing edge. The complete operating principle is described by Baumann and Bauer [23].

3.2 Test Parts

Polished shafts made of 100Cr6 steel with an 80 mm outer diameter were used as shaft counter faces. Even though the surface finish of these polished counter faces differs from plunge-ground ones, used in the most applications, they offer advantages when investigating the influence of the wetting properties on the wear of different sealing components. Hydrodynamic effects induced by surface structures can be kept low. Directional structures, which create a fluid transport in axial direction under rotation of the shaft, so-called lead, are avoided. In addition, the counter faces of the used shafts have the same roughness characteristics as far as possible. The measurement of the surface tension can be carried out directly on the counter faces without having to use specially manufactured test specimens. The hardness of the counter faces ranged from

56.3 HRC to 59.5 HRC. The surface roughness was between R_z 0.10 µm and 0.12 µm.

3.2.1 Shaft and Elastomer Materials

For the test bench investigations, radial lip seals of the type BAUM5X7 made of 75FKM585 with a sealing diameter of 80 mm were used (material properties by Freudenberg [24]). These are standard type radial lip seals according to DIN 3760/61 [25, 26] with an outer elastomer sleeve and a spring-loaded fluorine rubber sealing lip for high thermal and chemical requirements. These radial lip seals are largely inert to the lubricants used.

3.2.2 Lubricants

For this paper, investigations on eleven different lubricants were performed, consisting of five different base oils (mineral oils, poly-α-olefins, polyglycols, esters, and silicone oils). This includes lubricants that do not contain additives as well as lubricants that do. Tab. 1 lists the lubricants used. In the following, the respective lubricants are designated with the abbreviation given.

3.3 Pumping Rate Tests

To quantify how the different lubricants affect the active back-pumping rate of a radial lip sealing system, experimental pumping rate tests were carried out. These pumping rate tests can give an indication on the leak tightness of radial lip sealing systems [27, 28]. For these tests, the radial lip seals have been mounted inverse (the oil sump was located on the air side only) and the test chamber was filled with lubricant up to the center of the shaft. The test duration was 10 h and the oil sump temperature 40 °C. The revolution speed was a constant 1000 rpm, which corresponds to a sliding speed of 4.2 m s^{-1}. For each combination of lubricant three tests were carried out. Static and dynamic eccentricity have been measured before each test run and kept below 20 µm.

3.4 Wear Tests

The wear tests were carried out on the institute's 12-cell test bench [29]. The test duration was 100 h and the oil sump temperature 40 °C. The revolution speed was a constant 1000 rpm, which corresponds to a sliding speed of 4.2 m s^{-1}. For each lubricant, three tests were carried out. Static and dynamic eccentricity have been measured before each test run and kept below 20 µm. Leakage only occurred in conjunction with the silicone oil OSO with a total amount of < 1 g over the test duration.

4 Results

The results presented in this work are based on the analyses conducted in the AiF research project "Welleneinlauf" [1].

4.1 Material Values

4.1.1 Surface Tension of Shaft and Elastomer Materials

The three measuring liquids ethylene glycol, 1-bromo-naphthalene, and thiodiglycol were used to determine the surface tensions of the shaft counter faces and the elastomer. The measurements were carried out according to DIN55660-2 [16]. Fifteen drops of each measuring liquid were applied to each test material. To evaluate the contact angle, an image of every drop was recorded after t = 5 s. The mean values of the individual measured contact angels for every measuring liquid were used to calculate the surface tension. The surface tension for the

Table 1. Lubricants, viscosity at T = 20 °C [1].

Abbrev.	Manufacturer	Product name	Base oil	Additives	Viscosity [Pa s×10^{-3}]
FVA2	FVA	FVA2	Mineral oil	None	68.6
FVA3	FVA	FVA3	Mineral oil	None	270.4
PAO2	FVA	PAO2	Poly-α-olefin	None	140.4
PAO3	FVA	PAO3	Poly-α-olefin	None	576.5
PG1	FVA	PG1	Polyglycol	None	178.9
PG3	FVA	PG3	Polyglycol	None	627.8
MGP	Mobile	Glycoyle 22	Polyglycol	Yes	529.6
PX	Anonymized	Anonymized	Polyglycol	Yes	403.5
FCE	Fuchs	Cassida GLE-150	Ester	Yes	347.2
EX	Anonymized	Anonymized	Ester	Yes	405.9
OSO	OKS	1010/1	Silicone oil	None	104.8

100Cr6 steel counter faces were determined using the OWRK method. For the calculation of the surface tension of the low-energy 75FKM585 material, the method according to Wu was used. The calculated values for the surface tensions, as well as the corresponding disperse and polar fractions are listed in Tab. 2.

Table 2. Surface tension of shaft and elastomer material $T = 20\,°C$ [$Nm^{-1} \times 10^{-3}$].

	100Cr6	75FKM585
σ	41.1	19.3
σ_d	31.1	12.6
σ_p	10.1	6.7

4.1.2 Surface Tension of Lubricants

To determine the surface tension of the lubricants, a bubble pressure tensiometer was employed. The disperse and polar fractions of the surface tension were assessed by using the pendant drop method. Perfluoro octane served as a reference liquid. The measurements were carried out according to DIN55660-4 [21]. For each lubricant ten measurements were taken. The interfacial tension σ_{mean} against perfluoro octane, refer to the mean value of all measurements and the standard deviation σ_{std}, are listed in the Supporting Information S2. The disperse and polar fraction of the surface tension were determined using to the method of OWRK according to DIN55660-3 [30]. The values are given in Tab. 3.

The high polar fraction σ_p of the polyglycol-based lubricants compared to the other four base oils is clearly visible. The examined mineral oils and poly-α-olefins differ only slightly.

4.1.3 Spreading Coefficient

Based on DIN55660-2 [16], the spreading coefficients of all lubricant on 100Cr6 steel and 75FKM585 were calculated with the work of adhesion according to OWRK and are listed in the Supporting Information S3.

Regarding the sealing gap, the lubricant interacts with a metal surface (100Cr6 shaft) as well as an elastomer surface (75FKM585). To take this into account, the spreading coefficients for the two different solid surfaces must be considered in combination. For this purpose, the approach of a system spreading coefficient S_{SSYS} as an addition of the two spreading coefficients S_{100Cr6} and S_{FKM} is introduced in Eq. (13).

$$S_{SSYS} = S_{100Cr6} + S_{FKM} \tag{13}$$

The combined system spreading coefficients S_{SSYS} are listed in Tab. 4.

4.1.4 Penetrativity

The penetrativity Ψ of the different sealing systems was determined according to Eq. (11). Tab. 5 lists the values for sealing systems with FKM-RWDR. The measure the contact angles θ are listed in the Supporting Information S4.

4.2 Pumping Rate

To determine the pumping rate of the different sealing systems, each combination was tested three times and evaluated according to [1]. The mean values of the measured pumping rates are given in Tab. 6.

In order to classify the determined pumping rates, these can be compared to the values from Bekgulyan [28]. For his pumping rate measurements, he used plunge-ground counter faces instead of polished ones and tested them in combination with the lubricants FVA3, PAO3, and PG3, using the same type of radial lip seals made out of 75FKM585. The pumping rates shown in Tab. 6 are about 20 % lower than those described by Bekgulyan.

Table 3. Surface tension of lubricants $T = 20\,°C$ [$Nm^{-1} \times 10^{-3}$].

	FVA2	FVA3	PAO2	PAO3	PG1	PG3	MGP	PX	FCE	EX	OSO
Σ	32.1	32.8	26.8	31.9	36.4	39.8	33.1	33.8	30.7	32.5	21.1
σ_d	24.5	24.8	17.9	23.3	24.3	25.2	26.1	21.24	25.0	23.6	16.0
σ_p	7.6	8.0	8.8	8.5	12.1	14.6	7.0	12.56	5.7	8.9	5.1

Table 4. System spreading coefficients S_{SSYS} of lubricants for $T = 20\,°C$ [$Nm^{-1} \times 10^{-3}$].

	FVA2	FVA3	PAO2	PAO3	PG1	PG3	MGP	PX	FCE	EX	OSO
S_{SSYS}	–6.7	–8.0	5.5	–5.6	–14.4	–21.8	–9.5	–8.5	5.2	–6.7	10.4

Table 5. Penetrativity Ψ of different sealing systems for $T = 20\,°C$ [$m\,s^{-1}$].

	FVA2	FVA3	PAO2	PAO3	PG1	PG3	MGP	PX	FCE	EX	OSO
Ψ	1.36	1.52	1.47	1.55	1.49	1.55	1.54	1.53	1.53	1.53	1.44

Table 6. Pumping rate of lubricants [$g\,h^{-1}$].

FVA2	FVA3	PAO2	PAO3	PG1	PG3	MGP	PX	FCE	EX	OSO
1.01	1.41	2.04	2.84	2.05	3.00	3.02	2.60	1.87	3.42	1.47

4.3 Wear Tracks

To determine the depth and width of the shaft wear tracks, the shafts were measured by means of three tactile measuring traces, which are evenly distributed around the entire circumference, according to [1, 3]. The detected wear track width l_w and wear track depth h_d for the different sealing systems are listed in Tabs. 7 and 8.

4.4 Contact Width

To determine the contact width l_c of the sealing edge, the radial lip seals were photographed using an IMA-Sealobserver® in conjunction with a digital microscope. The photographs were evenly distributed around the entire circumference and evaluated according to [1]. The detected minimal and maximal contact widths $l_{c,min}$ and $l_{c,max}$ of the combinations are presented in Tab. 9.

As the maximum contact width $l_{c,max}$ of the sealing edge increases, wear becomes increasingly asymmetrical. This phenomenon has already been observed and described by Merkle [31] and Bauer [2] and does not depend on the test rig design, nor is it due to manufacturing errors in seal production or due to eccentricity deviations of the components. In the further course of this work, the maximum contact width $l_{c,max}$ of the sealing edge is used for correlation with the shafts wear track width l_w and wetting characteristics.

5 Correlation

First, the wear parameters of the counter faces, h_d and l_w, and the sealing edges $l_{c,max}$ are compared with each other. This provides insights about the wear of the individual sealing components and the sealing system as a whole. Two important questions need to be raised:

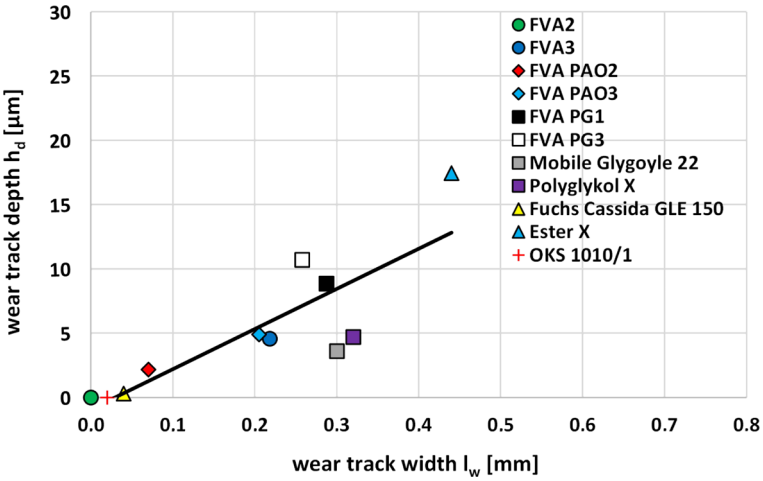

Figure 2. Relation between wear track depth h_d and width l_w of the sealing counter faces.

1. Do the wear track depth h_d and the width l_w of the counter face grow proportional to each other?
2. Do the counter face and the sealing edge wear to the same amount, or is one component more exposed to wear than the other?

To answer the first question, Fig. 2 compares the wear track depths h_d and the wear track widths l_w of the investigated counter faces. Across all the wear tests performed, a linear relationship with a correlation coefficient of $R = 0.85$ is obtained between the two parameters. The deeper the wear track on the counter face, the wider it becomes.

The second question can be answered by a comparison of the wear track depth h_d of the counter faces and the contact width $l_{c,max}$ of the sealing edges, shown in Fig. 3. Across all the wear tests performed, a linear relationship with a correlation coefficient of $R = 0.81$ is obtained between the two parameters. Contact widths $l_{c,max} < 0.16$ mm could not be found in any of the wear tests carried out. Likewise, wear of the counter face – wear track width l_w and wear track depth h_d – were observed only in combination with contact widths $l_{c,max} \geq 0.16$ mm. For small contact widths $l_{c,max} < 0.16$ mm, initial wear of the sealing edge is assumed, which is necessary to generate an active sealing mechanism and can therefore not be considered wear in the actual sense [2].

Due to the linear correlation of the individual wear parameters of the counter face and the sealing edge, the wear track depth h_d of the counter face is used as a measure for the wear of the sealing system as a whole in the further course of this work.

In order to show how functional properties of sealing systems can influence their wear, the wear track depth h_d is plotted against to the

Table 7. Shaft wear track width l_w of different sealing systems [m×10^{-3}].

	FVA2	FVA3	PAO2	PAO3	PG1	PG3	MGP	PX	FCE	EX	OSO
l_w	0.00	0.22	0.07	0.22	0.29	0.26	0.30	0.32	0.04	0.44	0.02

Table 8. Shaft wear track depth h_d of different sealing systems [m×10^{-6}].

	FVA2	FVA3	PAO2	PAO3	PG1	PG3	MGP	PX	FCE	EX	OSO
h_d	0.00	4.57	2.16	4.89	8.84	10.70	3.60	4.70	0.29	17.45	0.00

Table 9. Contact width l_c of different sealing systems [m×10^{-3}].

	FVA2	FVA3	PAO2	PAO3	PG1	PG3	MGP	PX	FCE	EX	OSO
$l_{c,max}$	0.15	0.29	0.17	0.28	0.34	0.27	0.31	0.37	0.25	0.46	0.17
$l_{c,min}$	0.13	0.25	0.15	0.25	0.27	0.24	0.25	0.29	0.22	0.31	0.14

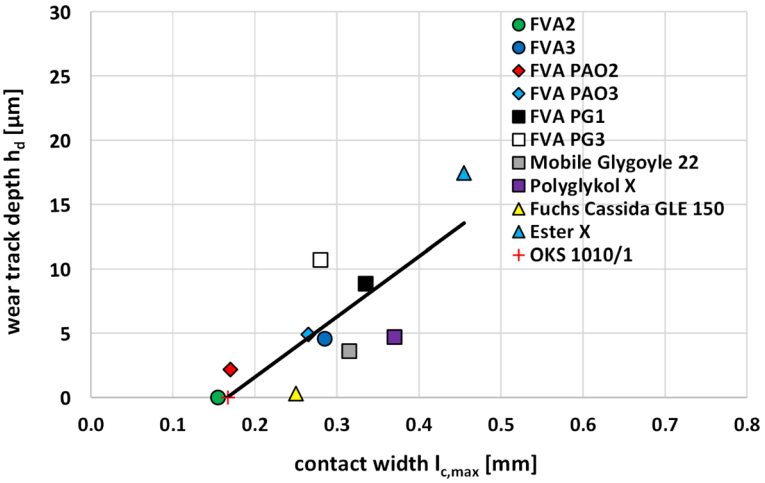

Figure 3. Relation between wear track depth h_d (counter face) and contact width $l_{c,max}$ (sealing edge).

pumping rate in Fig. 4. An increase in the pumping rate correlates to an increase in wear with a correlation coefficient of $R = 0.71$. Similar to the phenomenon of insufficient lubrication due to lead, described by Baumann [32], an increase in the pumping rate of the sealing system can lead to insufficient lubrication in the sealing contact. The consequence is an increase in solid contact between the counter face and sealing edge, which causes an increased wear of the sealing components involved. From this point of view, it must be concluded that a particularly high pumping rate increases sealing reliability on the one hand, but at the same time the higher wear limits the service life.

First promising approaches to predict the wear behavior of radial lip sealing systems using wetting properties were pursued by Klaiber [8] and Schuler [9]. Based on this work, Fricker [3] showed the relationship between wear of the sealing system and the spreading coefficients depending on shaft and sealing ring materials. In this work, a combined system spreading coefficient S_{SSYS} is introduced in Sect. 4.1.3 to describe the spreading behavior of a sealing system in one parameter.

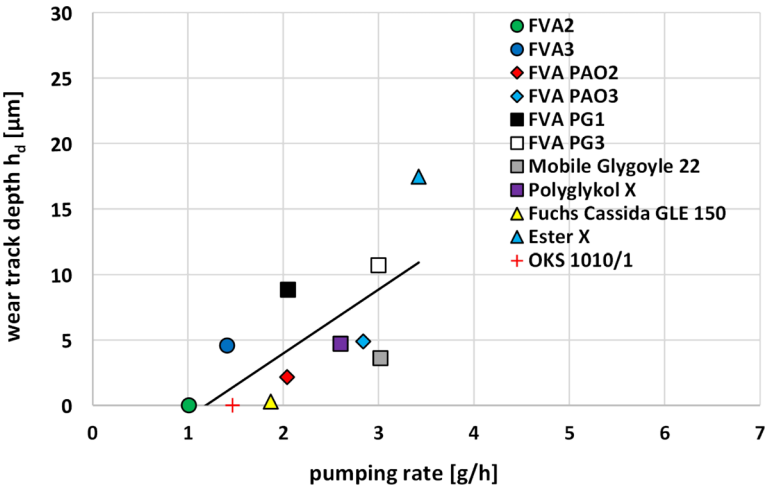

Figure 4. Relation between the wear track depth h_d and the pumping rate of the sealing system.

Fig. 5 shows the wear track depth h_d of the shaft counter faces plotted against the system spread coefficient S_{SSYS}. The detected wear track depth h_d increases with a decreasing system spreading coefficients S_{SSYS}. The combination with the lubricant Ester X deviates from this assumption. If these values are disregarded in the correlation, the correlation coefficient increases significantly from $R = 0.52$ to 0.77. Minor deviations can also be found in combination with Fuchs Cassida GLE 150. These two lubricants have an unknown additive composition. This could possibly lead to a significant change in the wear of the sealing components without majorly effecting the wetting properties, as shown by Klaiber [8].

Another wetting parameter to be considered in relation to wear on the sealing system is the penetrativity Ψ. A comparison of the wear track depth h_d and the penetrativity Ψ of the sealing systems is displayed in Fig. 6. With a decrease in penetrativity Ψ, the wear of the counter face increases. The calculated correlation coefficient is $R = 0.41$, which is quite low compared with the correlation of the system spreading coefficient. Especially in the range of low values, the wear track depth varies considerably for similar penetrativities Ψ. A low penetrativity Ψ can be an indicator of increased wear on the sealing system, but should be backed up by the assessment of other parameters, such as the pumping rate or the system spread coefficient S_{SSYS}.

6 Discussion

The research presented in this paper shows fundamental relationships between the wear of radial lip sealing systems, the spreading coefficient as well as the pumping rate of the sealing systems. If the wetting properties and the pumping rate tests are considered together, conclusions can be drawn about the tribological conditions in the sealing gap.

Sealing systems with an increased pumping rate show increased wear of the sealing components. This can be explained by regarding the functional principles of radial lip sealing systems summarized by Bauer [2]. The lubricant, brought into the sealing gap by the rotary motion of the shaft counter face, is pumped back to the oil side by an active back-pumping mechanism. This active back-pumping mechanism prevents leakage. While the lubricant is in the sealing gap, it causes the sealing edge to float. The sealing edge lifts off the counter face and thus reduces wear of the friction partners. If the system pumping rate is too high, more lubricant can potentially be brought back to the oil side than it is necessary for a sufficient lubrication of the sealing gap. Solid contact between the sealing edge and the counter face increments, which promotes increased wear.

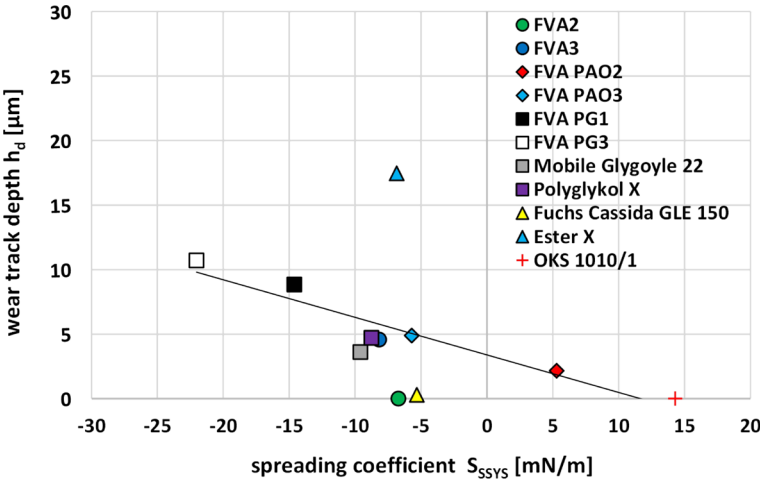

Figure 5. Relation between the wear track depth h_d and the system spreading coefficient S_{SSYS}.

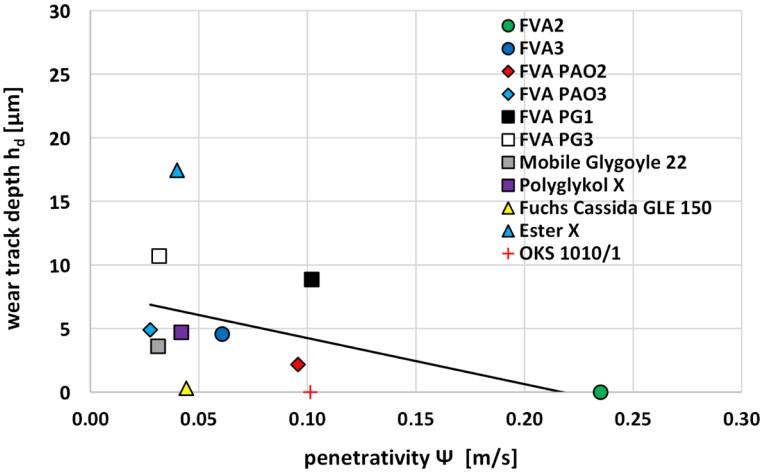

Figure 6. Relation between the wear track depth h_d and the penetrativity Ψ.

The wetting properties of the sealing components must also be included in this consideration. The ability of a lubricant to enter the sealing gap is determined primarily by the penetrativity. If more lubricant can penetrate into the sealing gap while the back-pumping potential remains the same, the pumping rate decreases. At the same time, more lubricant is available in the sealing gap and the wear of the friction partners is reduced. Once the lubricant has penetrated into the sealing gap, its bond to the counter face and the sealing edge is determined by the spreading coefficient. The higher the value, the stronger the lubricant bonds to the elastomer and the counter face. This increased bond reduces the pumping rate of the sealing system, but ensures a sufficient lubricating film between the friction partners and thus contributes to a reduction in wear.

Considering all these previously discussed observations, it must be noted that polished counter faces were used for all tests within this work. These deviate from plunge-ground counter faces which are mainly used in radial lip sealing systems. The polishing of the counter faces was necessary to be able to investigate the fundamental influence of the wetting properties on the wear of radial lip sealing systems. Possible unwanted hydrodynamic interactions, due to pronounced roughness structures on the counter faces, would have superimposed these effects and would have made the identification of them considerably more difficult.

It can be assumed that the correlations between the wetting properties and the wear on the polished shafts can be transferred to plunge-ground counter faces. However, it can be expected that these are less pronounced due to changes in hydrodynamics regarding the sealing gap. Nevertheless, the results show that it is quite expedient to use suitable and coordinated oil-elastomer-counter face combinations in order to construct stable and well-functioning sealing systems.

7 Summary and Conclusion

Modern lubricants, such as polyglycols and esters, cause problems when sealed with radial lip seals. Besides chemical incompatibility with the elastomer, increased wear and finally leakage can occur. The cause of these disadvantages compared to conventional, mineral oil-based lubricants is assumed to be in the wetting properties of the lubricants.

Different sealing systems were investigated to examine this behavior. Combinations of polished 100Cr6 steel counter faces, radial lip seals made of 75FKM585, and eleven chemically different lubricants (two mineral oils, four polyglycols, two poly-α-olefins, two esters, and one silicone oil) were examined.

The results indicate a correlation between the wear of the sealing systems and their wetting properties as well as the system pumping rate. The difference between the work of adhesion and the work of cohesion proved to be decisive. This difference is referred to as the spreading coefficient according to Harkins and Feldman [18] and is extended in this work to describe the lubricants spreading behavior in the radial lip sealing system.

Increased wear was observed especially in tests with polyglycol- and ester-based lubricants. These lubricants mostly show lower spreading coefficients than mineral oil-based lubricants. This leads to incomplete wetting, thus to a lubrication condition in the sealing gap which promotes abrasive wear and can have a negative influence on the service life.

Sealing systems with high pumping rates were also prone to excessive wear. These elevated pumping rates were mainly observed in combinations with polyglycols and esters. An increased pumping rate of the sealing system can lead to insufficient lubrication in the sealing contact. The consequence is an increase in solid contact between the counter face and sealing edge, which leads to an increased wear of the sealing components.

To reduce wear, negative system spreading coefficients and high pumping rates can be used to identify and avoid critical material combinations early in the design process as far as pos-

sible. If other material combinations are not possible, further wear-reducing strategies must be considered. Based on this work, a promising approach could be reducing the pumping rate of the sealing system.

Supporting Information

Supporting Information for this article can be found under DOI: https://doi.org/10.1002/ceat.202200375.

Acknowledgment

The IGF project 20111 N/1 of the Forschungskuratorium Maschinenbau e.V. (FKM) was funded by the AiF as a support of the Industrielle Gemeinschaftsforschung (IGF, Industrial Collective Research) by the Federal Ministry for Economic Affairs and Energy (BMWi) on the basis of a decision by the German Bundestag. Open access funding enabled and organized by Projekt DEAL.

The authors have declared no conflict of interest.

Symbols used

d_{cap}	[m]	capillary diameter
G	[–]	duty parameter
g	[m s^{-2}]	gravitation constant
h_d	[m s^{-2}]	wear track depth
h_t	[m]	immersion width
l_w	[m]	wear track width
l_c	[m]	contact width
$l_{c,max}$	[m]	maximal contact width
$l_{c,min}$	[m]	minimal contact width
p_m	[Pa]	average pressure in the sealing gap
$\hat{p}$	[Pa]	maximum pressure
Δp	[Pa]	pressure difference
r_1	[m]	radius
r_2	[m]	radius
S	[Nm$^{-1}\times10^{-3}$]	spreading coefficient
S_{100Cr6}	[Nm$^{-1}\times10^{-3}$]	spreading coefficient on 100Cr6
S_{FKM}	[Nm$^{-1}\times10^{-3}$]	spreading coefficient on FKM
S_{SSYS}	[Nm$^{-1}\times10^{-3}$]	system spreading coefficient
T	[°C]	temperature
W_a	[Nm$^{-1}\times10^{-3}$]	work of adhesion
W_c	[Nm$^{-1}\times10^{-3}$]	word of cohesion

Greek letters

η	[Pa s]	viscosity
θ	[°]	contact angle
θ_1	[°]	contact angle on surface 1
θ_2	[°]	contact angle on surface 2
σ	[Nm$^{-1}\times10^{-3}$]	surface tension
σ_a	[Nm$^{-1}\times10^{-3}$]	surface tension of material a
σ_{ab}	[Nm$^{-1}\times10^{-3}$]	interfacial tension
σ_b	[Nm$^{-1}\times10^{-3}$]	surface tension of material b
σ_d	[Nm$^{-1}\times10^{-3}$]	surface tension, disperse fraction
σ_l	[Nm$^{-1}\times10^{-3}$]	surface tension of a liquid
σ_p	[Nm$^{-1}\times10^{-3}$]	surface tension, polar fraction
σ_s	[Nm$^{-1}\times10^{-3}$]	surface tension of a solid
Ψ	[m s^{-1}]	penetrativity
ω	[rad s^{-1}]	angular velocity

Abbreviation

WORK	Owens, Wendt, Rabel, Kaeble

References

[1] P. Fricker, M. Baumann, F. Bauer, Welleneinlauf: Einfluss der Schmierstoffbenetzung auf den Verschleiß der Gegenlauffläche bei Radial-Wellendichtungen. Abschlussbericht FKM Vorhaben Nr. 612, IGF-Nr: 20111, Frankfurt am Main: FKM, **2021**, Forschungskuratorium Maschinenbau e.V. (FKM)

[2] F. Bauer, Federvorgespannte-Elastomer-Radial-Wellendichtungen: Grundlagen der Tribologie & Dichtungstechnik, Funktion und Schadensanalyse: Habilitation Teil 2/2, 1st ed., Springer, **2020**, Universität Stuttgart, Institut für Maschinenelemente.

[3] P. Fricker, M. Baumann, F. Bauer, *Wear* **2021**, *477 (5–8)*, 203897. DOI: https://doi.org/10.1016/j.wear.2021.203897

[4] T. Kretschmer, FVA-Sachstandsbericht "Gleitlagerbenetzung"/ IME: Technische Hochschule Aachen, **2007**.

[5] M. Kalin, I. Velkavrh, J. Vižintin, *Wear* **2009**, *267 (5–8)*, 1232–1240. DOI: https://doi.org/10.1016/j.wear.2008.12.072

[6] M. Kalin, M. Polajnar, *Tribol. Lett.* **2013**, *52 (2)*, 185–194. DOI: https://doi.org/10.1007/s11249-013-0194-y

[7] K. Bobzin, Einfluss der Schmierstoffbenetzung auf das Triboverhalten PVD beschichteter Maschinenelemente. AiF Forschungsbericht: AiF, **2010**, AiF Arbeitsgemeinschaft industrieller Forschungsvereinigungen "Otto von Guericke" e.V.

[8] M. Klaiber, Betriebs- und Benetzungseigenschaften im Dichtsystem Radial-Wellendichtung am Beispiel additivierter synthetischer Schmieröle, Dissertation, Universität Stuttgart, Institut für Maschinenelemente, **2013**, ISBN: 978-3-936100-50-1

[9] P. Schuler, Einfluss von Grenzflächeneffekten auf den Dichtmechanismus der Radial-Wellendichtung. Dissertation, Universität Stuttgart, Institut für Maschinenelemente, **2014**, ISBN: 978-3-936100-54-9

[10] S. Schmuker, W. Haas, Innovative Werkstoffe. Mit Radialwellendichtringen auf neuen, innovativen Wellenwerkstoffen und Beschichtungen zuverlässig abdichten. Abschlussbericht FKM Vorhaben Nr. 283, AiF-Nr. 15367 N/1, Frankfurt am Main: FKM, **2010**, Forschungskuratorium Maschinenbau e.V. (FKM).

[11] H.-D. Dörfler, *Grenzflächen und kolloid-disperse Systeme*, 1st ed., Springer, Berlin **2002**, ISBN 9783540425472.

[12] F. M. Fowkes, *Ind. Eng. Chem. Prod. Res. Dev.* **1964**, *56 (12)*, 40–52.

[13] D. K. Owens, R. C. Wendt, *J. Appl. Polym. Sci.* **1969**, *13 (8)*, 1741–1747.

[14] W. Rabel, *Farbe und Lack* **1997**, *77 (1971)*, 997–1005.

[15] D. H. Kaelble, *J. Adhes.* **1970**, *2 (2)*, 66–81.
[16] DIN 55660-2, Beschichtungsstoffe – Benetzbarkeit – Teil 2: Bestimmung der freien Oberflächenenergie fester Oberflächen durch Messung des Kontaktwinkels, Beuth Verlag GmbH, Berlin **2011**.
[17] S. Wu, *J. Adhes.* **1973**, *5 (1)*, 39–55.
[18] W. D. Harkins, A. Feldman, *J. Am. Chem. Soc.* **1922**, *44 (12)*, 2665–2685.
[19] K. L. Wolf, *Physik und Chemie der Grenzflächen, Band 1: Die Phänomene im Allgemeinen*, 1st ed., Springer, Heidelberg **1957**, ISBN 9783642494215.
[20] E. W. Washburn, *Phys. Rev. Lett.* **1921**, *17 (3)*, 273–283.
[21] DIN 55660-4, 2012, Beschichtungsstoffe – Benetzbarkeit – Teil 4: Bestimmung des polaren und dispersen Anteils der Oberflächenspannung von Flüssigkeiten aus einer Grenzflächenspannung, Beuth Verlag GmbH, Berlin **2011**.
[22] G. Ström, M. Fredriksson, P. Stenius, *J. Colloid Interface Sci.* **1987**, *119 (2)*, 352–361.
[23] M. Baumann, F. Bauer, Moderne visuelle Untersuchungsmethoden für die Verschleißanalyse am Beispiel Radial-Wellendichtring, 20th Int. Sealing Conf. (ISC), Stuttgart, Oktober **2018**; Fluidtechnik; Frankfurt am Main: Fachverband Fluidtechnik im VDMA e.V, 2018, S. 93–104 - ISBN 978-3-8163-0727-3.
[24] Freudenberg Forschungsdienste KG: Elastomere Werkstoffe, **2001**.
[25] DIN 3760, Radial-Wellendichtringe, Deutsches Institut für Normung e.V., Berlin **1996**.
[26] DIN 3761, Radial-Wellendichtringe für den Maschinenbau (NA 060-36-74 AA), DIN-Normenausschuss Maschinenbau Fachbereich Fluidtechnik **2018**.
[27] M. Remppis, Untersuchungen zum Förderverhalten von Dichtsystemen mit Radial-Wellendichtringen aus Elastomer, *Dissertation*, Universität Stuttgart, Institut für Maschinenelemente **2016**, ISBN 978-3-936100-68-6
[28] S. Bekgulyan, F. Bauer, W. Haas, Berechenbare Dichtgüte II. Rechnerische Abschätzung der Dichtgüte von Radial-Wellendichtungen durch Kenntnis der Systemparametereinflüsse II. Abschlussbericht FVA Vorhaben Nr. 617 II, IGF-Nr. 17938 N/1, Forschungsvereinigung Antriebstechnik e.V. (FVA), Frankfurt am Main **2017**.
[29] Universität Stuttgart, Institut für Maschinenelemente: Wellendichtungen 24-Zellen-Dauerlaufprüfstand. Universität Stuttgart, Institut für Maschinenelemente (Hrsg.), IMA-TechSheet, V1, #101010, Stuttgart **2021**.
[30] DIN 55660-3, Beschichtungsstoffe – Benetzbarkeit – Teil 3: Bestimmung der Oberflächenspannung von Flüssigkeiten mit der Methode des hängenden Tropfens, Beuth Verlag GmbH, Berlin **2011**.
[31] L. Merkle, M. Baumann, F. Bauer, Influence of Alternating Temperature Levels on the Wear Behavior of Radial Lip Seals, Test Rig Design and Wear Analysis, **2021**, 163–164. ISBN 978-86-6060-073-0.
[32] M. Baumann, Abdichtung drallbehafteter Dichtungsgegenlaufflächen – Messung, Analyse, Bewertung und Grenzen, *Dissertation*, Universität Stuttgart, Institut für Maschinenelemente **2017**, ISBN 978-3-936100-69-3.

